

# Modeling Thermal Regeneration of Wall-Flow Diesel Particulate Traps

Grigorios C. Koltsakis and Anastasios M. Stamatelos

Laboratory of Applied Thermodynamics, Aristotle University Thessaloniki, 540 06 Thessaloniki, Greece

*Stricter emission control legislation for diesel use has been increasing interest in highly efficient wall-flow particulate filters. The mathematical modeling of the filter regeneration process is indispensable in developing reliable and durable trap systems for various applications. Although modeling of wall-flow filters has been investigated extensively, significant problems still exist in the correlation of modeling results with measurements. This article describes an improved modeling and model tuning approach. A classical zero-dimensional regeneration model, modified to account for incomplete soot oxidation effects, is discussed, and existing and novel methods of estimating trap loading, crucial in all modeling applications, are compared. The design of a model tuning approach based on full-scale experiments is highlighted with examples of model predictions during trap failure that show capabilities of supporting the design of trap protection techniques. Applications to regeneration rate control, filter sizing and the development of on-board diagnostics are demonstrated with examples. Dimensional analysis is used for the concise quantitative evaluation of the parameters affecting the evolution of the regeneration process.*

## Introduction

The interest in diesel engine exhaust after-treatment systems is expected to increase with stricter U.S. and European emission legislation amendments planned for the near future. The wall-flow particulate filter is the most efficient device for reducing diesel soot emissions, attaining filtration efficiencies of the order of 90% at nominal operation conditions (Johnson et al., 1994). Specific application problems related to filter durability have limited their use mainly to city buses, delivery trucks, and forklift trucks. Further work is needed to develop trap systems suitable for a wider application to commercial vehicles or passenger cars (Merrion, 1994).

The particulate trap concept has focused intensive research and development activities around the world, and a variety of systems are offered by various manufacturers (Hoepke, 1989; Stamatelos, 1991; Pattas et al., 1990; Rao and Cicanek, 1994). Any trap oxidizer system is based on a durable temperature resistant filter (the trap) which removes particulate matter from the exhaust before it is emitted to the atmosphere. The accumulated particulate raises trap backpressure that is, the pressure difference across the trap necessary to

force the exhaust through it. The typical backpressure level varies with a different type of traps, and increases as the trap becomes loaded with particulate. High backpressure is undesirable, since it increases fuel consumption and reduces available power. It is necessary to clean the trap periodically by burning off (oxidizing) the collected particulate. This process is known as regeneration (Weaver, 1984; Howitt and Montierth, 1981).

A significant soot oxidation without catalytic aids starts at temperatures between 500 and 600°C depending on exhaust flow rate and oxygen content. Exhaust temperatures of that order are observed only at high load operation of the diesel engine. They are scarcely attained in the driving cycles of the official tests (ECE-EUDC, FTP-75, etc.). Thus, special regeneration techniques that fall into three broad categories are employed (Lox et al., 1991):

- Thermal regeneration by use of engine measures or by the supply of external energy
- Catalytic regeneration (catalytically coated filter or fuel doping)
- Aerodynamic regeneration (using compressed air to remove the soot).

Correspondence concerning this article should be addressed to A. M. Stamatelos.

The evolution of the soot combustion reaction in the first two categories of techniques is strongly affected by the exhaust gas conditions; high reaction rates may result in too high temperatures and possibly filter failure. The problem of controlling efficiently the thermal regeneration rate is today the major obstacle for the wider application of particulate traps. The design of regeneration control systems must be supported by reliable mathematical modeling of the thermal regeneration process. Also, sizing and general design optimization of vehicle trap systems is a task that requires extensive modeling work.

Significant research work during the last decade, focused on modeling thermal regeneration of particulate filters. The problem is very complicated, and significant difficulties exist in exploiting laboratory results (thermogravimetry) in the estimation of kinetics parameters applicable to full-scale models (Pattas and Michalopoulou, 1992; Hoffmann and Ma, 1990). For this reason, a special engineering approach to the modeling problem has proven more effective. This approach is described in detail in this article. It must be emphasized that the approach comprises two equally important parts:

- The mathematical formulation of the model
- The formulation of a specific tuning methodology.

This second tuning part is required in order to allow a relatively simple model to represent full-scale results with real trap systems. The tuning part is supported by a number of computational tools that assist the exploitation of full-scale experimental results in the estimation of critical model parameters.

In reference to the above, the main contribution described in this article is related to the adoption of a sound and simple thermal regeneration model (Bissett and Shadman, 1985) with some improvements in the reaction kinetics section, and the formulation of a full methodology for its exploitation in representing real-world trap regeneration behavior. A novel approach for the estimation of trap loading based on energy balance calculations during regeneration is incorporated in the tuning methodology. The results are presented in dimensionless form and exploited as design rules.

An important reason for adopting this simple zero-dimensional approach is its suitability for extension to model catalytic regeneration. This forms the subject of a future article which is considered as a followup to this one, covering the very complex problem of regeneration assisted by catalytic fuel additives.

## Modeling Thermal Trap Regeneration

Since research on the application of trap systems started more than 10 years ago, there already exists a fairly large number of computer models for thermal regeneration of cellular ceramic filters. Here one must mention first the classical work of Bissett and Shadman (1985) with a zero-dimensional model, along with its extension to a one-dimensional (1-D) model of a trap channel (Bissett, 1984). However, only relatively limited application of this model to real-world applications has been presented so far (McCabe and Sinkevitch, 1986). Other researchers also presented regeneration models later on (Garner and Dent, 1988; Pattas and Samaras, 1989; Pauli et al., 1984). Recently, a quasi-1-D model based on the one due to Bissett was extended to 2-D (axisymmetric) and

coupled with an FEM stress analysis program to analyze thermal stresses in the filter (Aoki et al., 1993). However, it seems that the necessity still exists for a sound thermal regeneration model, tunable to real-world conditions and able to support the design of regeneration control systems. Such a model should obviously rely on accurate and realistic kinetics scheme and data, as well as on reliable thermophysical properties data for the ceramic and soot. The control-oriented regeneration model adopted in this work is based on the well-established zero-dimensional approach of Bissett and Shadman (1985) chosen for its simplicity and soundness in its mathematical foundations, allowing the inclusion of more complex kinetic schemes for an extension to catalytic regeneration which is currently underway.

The model considers that the exhaust gas flows through two layers: the particle deposit, which shrinks uniformly with time during regeneration, and the porous ceramic channel wall (Figure 1). This simplifying model construction employs a single spatial variable  $x$ , whereas all variations in the direction perpendicular to  $x$  are neglected. The uniform soot deposition assumed over the monolith channels is expected since the combined flow resistance of the porous wall and soot deposit is typically much greater than the flow resistance of the open monolith channels. The assumption of equal exhaust gas temperature entering the deposit layer over the monolith channels is realistic for sufficiently high exhaust flow rates related to the monolith volume, considering that the conductive heat transfer between the channel gas and the monolith walls is negligible compared to convective transport in the channels. This has been also proven experimentally by Lep-perhoff and Kroon (1984).

Typical diesel particulate consists mainly of a carbonaceous core (soot formed during combustion), adsorbed compounds such as unburnt and partially oxygenated hydrocarbons, sulfates (due to the oxidation of the sulfur contained in the fuel), and metal oxides (Huehn and Sauerteig, 1989; Moser et al., 1990). The solid part and the adsorbed hydrocarbons readily react with oxygen present in the exhaust gas at sufficiently high temperatures (over 500°C). However, in the most mathematical models for diesel particulate traps, it is assumed that the soot oxidation reaction can be represented by the complete carbon oxidation. Several works

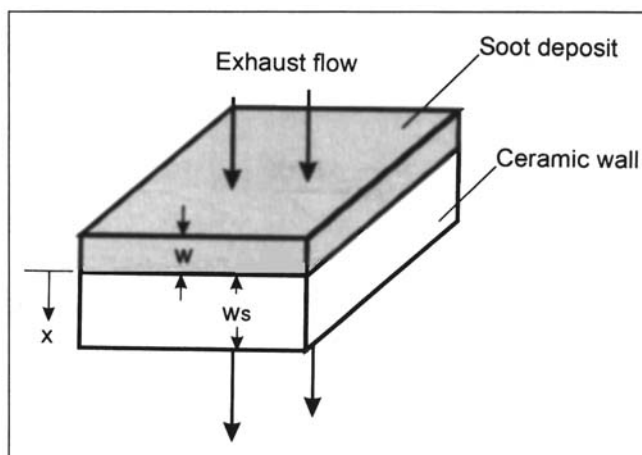
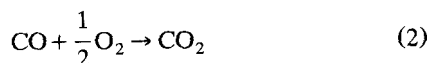


Figure 1. Model geometry for a section of the filtration area of a wall-flow monolithic trap.

(Johnson et al., 1994) have shown that carbon monoxide is present in significant quantities in the reaction products. Considering the relatively high reaction enthalpy of CO oxidation, it is expected that the extent of soot incomplete oxidation could play an important role in the reaction heat released during regeneration which affects the entire regeneration process.

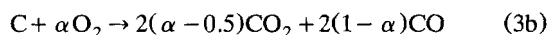
In this work, the kinetics submodel of the Bissett and Shadman (1985) approach is modified to account for incomplete soot oxidation. In reality, carbon gasification is a two-step process



However, at the present stage we could not employ such a two-step scheme, because we lack sufficient kinetic and internal diffusion data for the evolution of these processes in the specific and very complex type of reactor. Additionally, because of both external and internal burning rates, soot gasification could alter the internal pore-size distribution of the soot layer, and thus fundamentally affect burnout rate. In order to overcome these problems, we keep the shrinking layer assumption and lump the unknown kinetics and internal diffusion parameters in an apparent one-step kinetic scheme taking into account incomplete oxidation based on the following reaction



or



where  $\alpha$  is an index of the completeness of the reaction taking values from 0.5 to 1. The parameter  $\alpha$  should, however, be estimated beforehand. It must be mentioned that this estimation can be performed with good accuracy for the most practical cases of interest. A methodology for the assessment of the index  $\alpha$ , based on routine regeneration experimental results with simple temperature recordings, will be presented in the following section.

Mass exchange between exhaust gas flow and reactants or products is negligible compared to the exhaust flow itself. The conservation of mass for the exhaust gas can then be expressed as

$$\rho v = \frac{F(t)}{A} \quad (4)$$

Assuming that the reaction (Eq 3) is first-order in  $O_2$  and that diffusion is negligible compared to convection, the oxygen balance equation is

$$\frac{\partial}{\partial x}(\rho v y) = -s_j k_j \rho y \alpha \quad j = 1, 2 \quad (5)$$

where subscript  $j$  identifies regions 1 and 2. Since there is no reaction in region 2 (porous wall),  $k_2 = 0$ . The coefficient  $k_1$

for region 1 (deposit) is calculated from the following rate expression

$$k_1 = kT e^{-E/RT} \quad (6)$$

For the apparent activation energy  $E$  appearing in Eq. 6, several values have been proposed ranging from 80 to 160 kJ/mol (Pattas and Michalopoulou, 1992; Bissett, 1984; Pauli et al., 1984; Hoffmann and Ma, 1990). Experimental evidence (Lep-perhoff and Kroon, 1984; Pattas et al., 1995; Pattas and Michalopoulou, 1992) implies that a value of 150 kJ/mol satisfactorily represents regeneration reaction behavior. Having adopted a value for the apparent activation energy, the factor  $k$  can be tuned accordingly to obtain good agreement between calculations and measurements. Such a procedure is described in the following sections.

Assuming that the gas temperature equals that of the solid phase very near the entrance region of the deposit layer and considering negligible heat losses to the surroundings, the energy conservation equation can be formulated as below

$$\rho_j C_{pj} \frac{\partial T}{\partial t} = s_j \left( -\frac{\Delta H}{M_\alpha} \right) k_j \rho y + \frac{\partial}{\partial x} \left( \lambda_j \frac{\partial T}{\partial x} \right) - \rho v C_{pg} \frac{\partial T}{\partial x} \quad j = 1, 2 \quad (7)$$

$\Delta H$  indicates a combined reaction enthalpy resulting from the complete and incomplete oxidation of carbon, which is linked to  $\alpha$  according to the relation

$$\Delta H = 2(\alpha - 0.5)\Delta H_{(i)} + 2(1 - \alpha)\Delta H_{(ii)} \quad (8)$$

The rate of shrinkage of the deposit layer is proportional to the rate of oxygen consumption and inversely proportional to oxidation efficiency index  $\alpha$

$$\rho_1 \frac{dw}{dt} = \frac{M_c}{M_\alpha} \frac{F(t)}{A} [y(x=0) - y(x=-w)] \frac{1}{\alpha} \quad (9)$$

The initial conditions for the system (Eqs. 5, 7 and 9) are

$$T(x, t=0) = T_b \quad (10)$$

$$w(t=0) = w_b \quad (11)$$

The boundary conditions at  $x = -w$  are

$$y = y_i(t) \quad (12)$$

$$\lambda_1 \frac{\partial T}{\partial x} = \rho v C_{pg} [T - T_i(t)] \quad (13)$$

where  $F(t)$ ,  $y_i(t)$ , and  $T_i(t)$  are the known conditions of the exhaust gas. At  $x = w_s$

$$\frac{\partial T}{\partial x} = 0 \quad (14)$$

Using the dimensionless variables, the system can be written as follows for  $-\bar{w} < \bar{x} < \bar{w}_s$ ,  $\bar{x} \neq 0$

$$\bar{F} \frac{\partial y}{\partial x} = \frac{-\bar{k}_j(\bar{T})y\alpha}{\bar{T}}, \quad j=1,2 \quad (15)$$

$$\bar{C}_{pj} \frac{\partial \bar{T}}{\partial t} = \frac{1}{\epsilon} \frac{\partial}{\partial \bar{x}} \left( \bar{\lambda}_j \frac{\partial \bar{T}}{\partial \bar{x}} \right) + \frac{\Delta H \bar{k}_j(\bar{T})y}{\bar{T}} - \bar{F} \frac{\partial \bar{T}}{\partial \bar{x}}, \quad j=1,2 \quad (16)$$

$$\frac{d\bar{w}}{dt} = \bar{M}\bar{F}y \Big|_{-\bar{w}}^0 \frac{1}{\alpha} \quad (17)$$

with the boundary conditions for  $\bar{x} = -\bar{w}$

$$y = y_i \quad (18)$$

$$\frac{1}{\epsilon} \frac{\partial \bar{T}}{\partial \bar{x}} = \bar{F}(\bar{T} - \bar{T}_i) \quad (19)$$

and for  $\bar{x} = \bar{w}_s$

$$\frac{\partial \bar{T}}{\partial \bar{x}} = 0 \quad (20)$$

The solution method for the above system of equations is presented by Bissett and Shadman (1985). The solution is obtained by perturbation expansions of  $\bar{T}$ ,  $y$ ,  $\bar{w}$  in the same parameter  $\epsilon$ . For example

$$\bar{T} = T_0 + \epsilon T_1 + \epsilon^2 T_2 + \dots \quad (21)$$

For typical parameter values,  $\epsilon$  takes values of the order of  $10^{-3}$ . It is therefore a very good approximation to solve only for the leading-order terms of  $\bar{T}$ ,  $y$ ,  $\bar{w}$ . Moreover, it can be shown that  $T_0$  is independent of  $x$ . Following the solution method of Bissett and Shadman (1985) and taking into account the incomplete oxidation terms introduced above, the dynamic behavior of the leading-order terms is expressed by the following equations

$$y_0 = \begin{cases} y_i \exp \left[ -\frac{\bar{k}(T_0)}{T_0 \bar{F}} \alpha (\bar{x} + w_0) \right], & \bar{x} \leq 0 \\ y_i \exp \left[ -\frac{\bar{k}(T_0)}{T_0 \bar{F}} \alpha w_0 \right], & \bar{x} > 0 \end{cases} \quad (22)$$

$$\frac{dT_0}{dt} = \frac{\bar{F}(\bar{i})}{\bar{C}_{p1}w_0 + \bar{C}_{p2}\bar{w}_s} \cdot \left\{ \frac{\Delta H y_i(\bar{i})}{\alpha} \left[ 1 - \exp \left( -\frac{\bar{k}(T_0)w_0}{T_0 \bar{F}} \alpha \right) \right] + \bar{T}_i(\bar{i}) - T_0 \right\} \quad (23)$$

$$\frac{dw_0}{dt} = -\bar{M}\bar{F}(\bar{i})y_i(\bar{i}) \frac{1}{\alpha} \left[ 1 - \exp \left( -\frac{\bar{k}(T_0)w_0}{T_0 \bar{F}(\bar{i})} \alpha \right) \right] \quad (24)$$

Equations 23 and 24 can be solved numerically by Runge-Kutta 4th-order techniques with the initial conditions

$$T_0 = w_0 = 1 \quad (25)$$

## Trap Loading Estimation Methodologies

A usual problem arising in the simulation of particulate traps regeneration using computer models is the assessment of the mass of the accumulated soot. It is essential to have a realistic estimation of the filter loading, since the regeneration process is sensitive to this quantity in regard to both temperature evolution as well as regeneration duration, as will be discussed in the following section. A good estimation of the filter loading is also necessary when employing experimental results for the tuning of the model kinetic parameters to match real-world soot oxidation characteristics. Weighting of the clean and the loaded filter provides the more direct method to estimate the deposit mass; it presents, however, practical difficulties: the presence of moisture in the ceramic filter during the assembly may lead to significant errors in the estimation of soot weight. Moreover, the clean and the loaded filter should have the same moisture content in the ceramic, which is difficult to assure in most cases. In practice, a number of indirect techniques are employed and are discussed below:

- Measurement of particulate emissions before and after the trap during the loading phase
- Correlation of trap loading with backpressure data
- Energy balance calculations.

Apart from the above general categories, a specially designed technique based on the absorbance of electromagnetic (RF) energy from the loaded filter has also been designed for the on-line measurement of diesel particulate loading (Walton et al., 1991). The amount of RF energy absorbed by a material is proportional to its dielectric loss factor. The dielectric factor of cordierite is negligible compared to that of the accumulated soot. Thus, absorbance of RF energy, measured by two probes (transmitter and receiver) positioned upstream and downstream the filter provides an indication of soot loading at any time.

The trap loading by measuring instantaneous particulate emissions is obtained by a simple mass balance. The procedure is direct and simple, but requires demanding instrumentation for the accurate measurement of particulate emissions before and after the trap (Lepperhof and Kroon, 1984).

Backpressure techniques are widely used for trap system control and safety purposes on vehicle. The trap backpressure is a complex function of trap loading, exhaust gas flow rate and temperature. Other factors may also play an important role, such as the nature and composition of the accumulated particulate. For practical purposes, trap backpressure is used as an indication of maximum permissible trap loading on-road by means of rule of thumb approaches (Weaver, 1984; Higuchi et al., 1983; Wade et al., 1983; Shadav et al., 1984). The lack of knowledge of the effect of soot composition and accumulation mode on backpressure characteristics limits the accuracy obtainable by this technique. Moreover, such estimations must be based on the assumption of uniform soot deposition in all trap channels radially and axially. This as-

sumption may, however, induce significant errors, especially during the regeneration process (Wiedemann et al., 1983).

Taking into account the above mentioned difficulties, a plausible methodology for trap loading estimation could alternatively be supported by energy balance calculations. The control volume selected for these calculations encloses the trap and cuts the system in two points, namely, the inlet and outlet section. The resulting energy balance takes the following form

$$\dot{H}_{in}(t) - \dot{H}_{out}(t) = \frac{dU_{trap}}{dt} - \Delta H \frac{dm_{soot}}{dt} \quad (26)$$

where  $\Delta H$  denotes a composite enthalpy of reaction for the combination of the two soot oxidation reactions, as explained above.

Equation 26 can be integrated over a full regeneration with the engine operating at a steady-state point. The integration can be performed also during unsteady engine operation, provided that the trap is thermally stabilized before and after the integration time at known temperatures. The calculation implies the following realistic assumptions:

- It is assumed that at usual thermal (noncatalytic) regeneration temperatures any soluble organic part previously accumulated has already been desorbed and does not contribute in the regeneration exothermal process.
- The total duration of the experiment is sufficient for the trap to stabilize at a constant temperature (usually equal to that of the feed exhaust gas) to calculate the respective internal energy term in Eq. 26.

Equation 26 implies that the above methodology requires continuous flow rate, temperature recordings (before and after the trap) during the regeneration process, as well as an estimation of the parameter  $\alpha$  indicating the percentage of soot oxidized to CO. This parameter can be calculated by measurements of CO emissions before and after the trap.

An example is presented in Figure 2. The exhaust gas flow rate for this measurement was kept constant at  $40 \times 10^{-3}$  kg/s. The first graph shows the evolution of exhaust gas temperature before and after the trap. By integration, we get the

lefthand side terms of the balance Eq. 26. The initial trap temperature is 410°C. After completion of the regeneration process, the temperature after the trap approaches asymptotically that before the trap and stabilizes finally at about 710°C. The trap temperature change provides directly the internal energy variation term of Eq. 26. The quantity  $\Delta m_{soot} \Delta H$  can now be directly calculated, but the individual terms of this product remain unknown.

In the second graph the CO emissions recordings before and after the trap are plotted. Integrating  $F(t)$  ( $[CO]_{out} - [CO]_{in}$ ) over time, we obtain the total CO emitted due to incomplete soot oxidation, which equals in this case approximately 17 g. The parameter  $\alpha$  can now be found using a trial-and-error procedure, as shown below

$$\alpha \xrightarrow{\text{Eq. 8}} \Delta H \xrightarrow{(\Delta H)(\Delta m) = \text{known}} \Delta m \xrightarrow{\text{Eq. 1, } \alpha} CO \quad (27)$$

Following this procedure for the example presented in Figure 2, it is found that  $\alpha = 0.8$ , and  $\Delta m = 18$  g. The trap loading for this case measured by the mass balance technique was assessed to be between 15 and 17 g.

As regards the value of  $\alpha$ , experience with a number of available thermal regeneration CO recordings has shown that the value determined above is relatively insensitive to regeneration conditions. This is confirmed by other researchers in the field (Aoki et al., 1993). The sensitivity of this parameter is much more enhanced in catalytic regeneration (De Soete, 1987).

The experiment presented above is simulated by means of the computer model. Two runs are conducted in order to assess the importance of taking into account incomplete oxidation and CO formation during the regeneration process. The results presented in Figure 3 clearly illustrate that the assumption of complete soot oxidation to  $CO_2$  may lead to remarkably different solutions that in our case overestimate the maximum developed temperature.

The energy balance equation can also be employed in the opposite direction, namely, in the estimation of the percentage of soot oxidized to CO (when CO measurements are not available), provided that the initial trap loading is known.

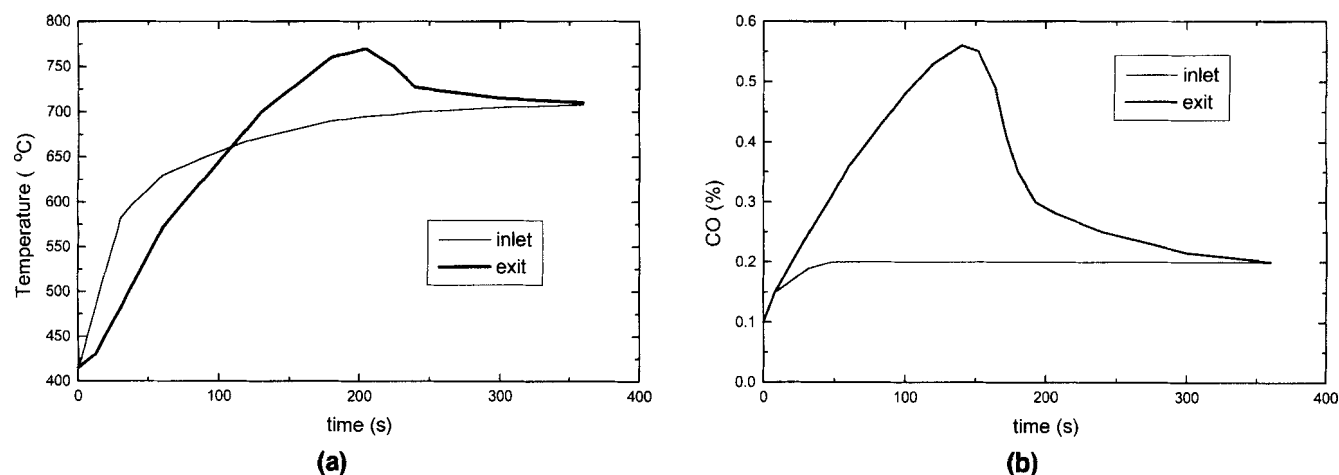


**Figure 2. Estimation of trap loading by energy balance calculations.**

The first graph shows the evolution of exhaust gas temperature before and after the trap. In the second graph the CO emissions recordings before and after the trap are plotted. The exhaust gas flow rate is kept constant at 40 g/s;  $O_2$  concentration in the exhaust is 2.5%.

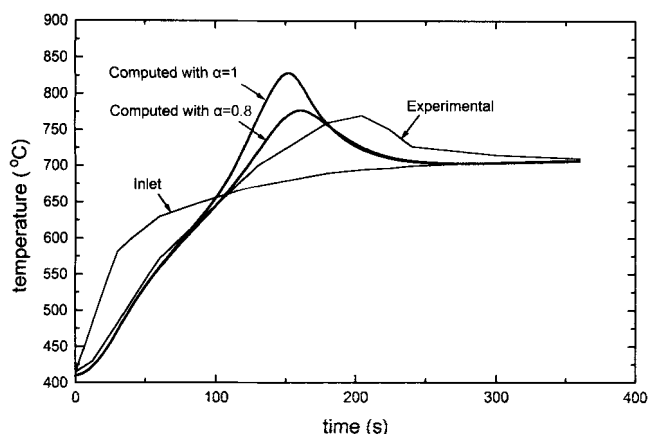


**Figure 3. Influence of incomplete soot oxidation on model results.**

The predicted temperatures after the filter are compared assuming: (a) complete oxidation; (b) incomplete oxidation. They are compared with the experimentally measured temperature.

### Tuning to Full-Scale Regeneration Experiments

As mentioned in the modeling section, a number of laboratory works are known concerning the determination of the pertaining kinetic parameters of diesel soot combustion (Pauli et al., 1984; Frohne et al., 1989; Hoffmann and Ma, 1990; De Soete, 1987). Significant discrepancies exist among laboratory measurements of the kinetic parameters due to the following reasons:

- (1) Differences in behavior of soot combustion in laboratory setup (such as thermogravimetry) compared to a real world experiment (diesel filter subjected to exhaust gas flow).
- (2) Differences in mean-size distribution and soluble organic fraction (SOF) of soot particulates tested. As well known, particulate size significantly affects internal diffusion and many hydrocarbon fractions burn up readily at lower temperatures than the solid part, thus initiating the soot oxidation.
- (3) Lack of data concerning the percentage of soot oxidation to CO.

In fact, the procedure followed for the purpose of the present work is based on a well accepted value for the apparent activation energy ( $E$ ) of 150 kJ/mol, whereas the value of the collisions factor frequency factor ( $k$ ) can be tuned by a series of full-scale experiments, like that reported in Lepperhof and Kroon (1984). Comparisons between computed and measured regenerations are presented in this section.

The experimental measurements employed for tuning purposes were conducted in the frame of a German auto-manufacturers association (FVV) study (Lepperhof and Kroon, 1984). A Mercedes 240D vehicle equipped with a particulate

**Table 1. Technical Data of the Particulate Filter Used in the Experiments and Model Applications**

Cell Density	100 cells/in. <sup>2</sup>	Wall Thickness	0.43 mm
Diameter	188 mm	Filter Material	Cordierite
Length	152 mm	Porosity	50%

SI unit: mm<sup>2</sup> = in.<sup>2</sup> × 645

**Table 2. Test Conditions for Comparison of Experimental with Model Results**

Test case	$T_i$ °C	$m_b$ g	$F$ g/s	$\Delta P$ kPa	$y_i$ %
1	680	16	40	35	8.1
2	680	14	40	35	2.4
3	670	17	22	20	7.5
4	690	32	40	55	4.8

filter was used. A variety of regeneration conditions were realized by the use of a heat exchanger and an oxygen injector located above the trap. Technical data for the particulate filter are given in Table 1.

Four different test cases will be presented and compared with experimental measurements to evaluate model prediction capabilities under a variety of flow and temperature conditions. The test conditions are tabulated in Table 2. According to the discussion in the previous section, a constant value of  $\alpha = 0.8$  is kept in all computations.

Test case 1 represents a typical regeneration under moderate flow rate and loading conditions. The comparison of the experimentally measured trap exit temperature with the predicted one is shown in Figure 4. The correlation observed is fairly good for the purposes of the model, while keeping in mind the relative uncertainties regarding some of the input parameters used. The zero-dimensional model seems to work also well for the case of a regeneration with low oxygen content of the exhaust gas. Figure 5 shows a regeneration at oxygen concentration of 2.4%, a value which is observed during operation at full load conditions with low A/F ratios. Test case 3 is a regeneration at relatively low flow rate. Still, the results presented in Figure 6 show good agreement of the model with the reality apart from a 50°C underestimation of the maximum temperature. Obviously, the flow rate used was not sufficiently low to cause significant temperature gradients along the trap channels that would counter the model assumptions. The last test (Figure 7) is performed with a signif-

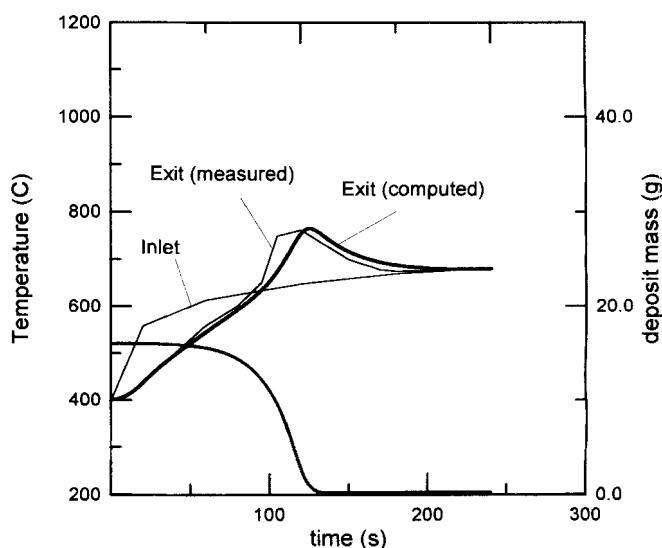


**Figure 4. Regeneration at moderate flow and trap loading conditions (test case 1).**

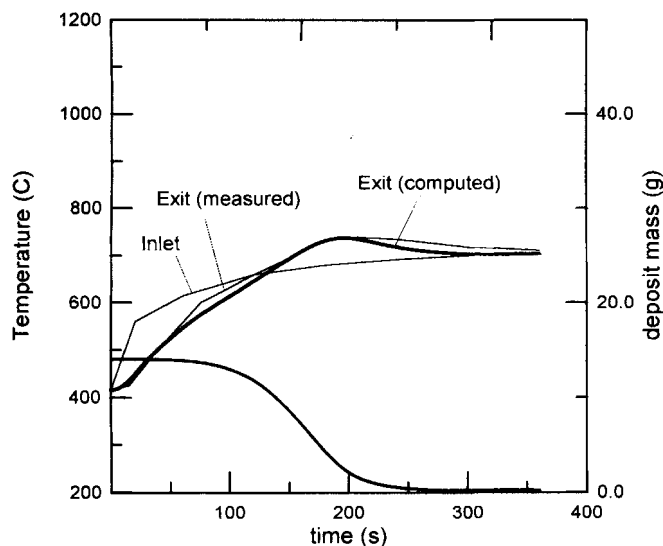


Figure 5. Regeneration at very low oxygen concentration of the exhaust gas (test case 2).

icantly higher initial loading of the filter. The agreement between the calculated and the measured temperatures is also satisfactory in this case.

### Dimensional Analysis of the Regeneration Process

The prediction of the regeneration process by use of the mathematical models provides useful hints in order to assess the importance of various design and operation parameters. As an example, the danger from trap overheating during different driving scenarios can be assessed by predicting the maximum temperature developed in each case. In this section the dimensional analysis will be applied to a typical re-

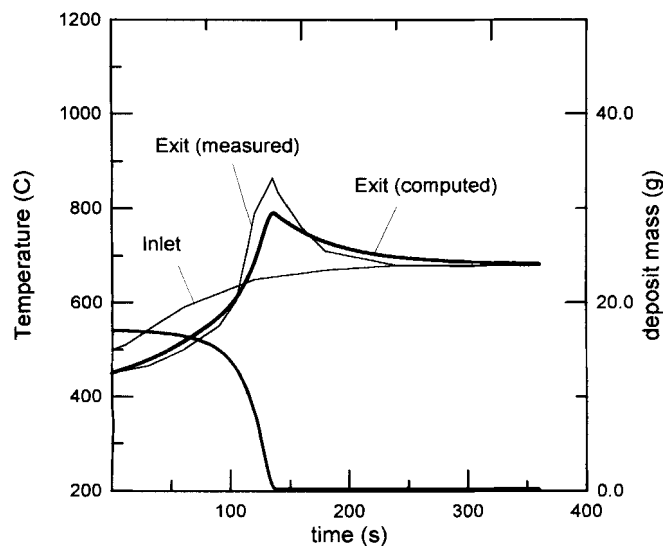


Figure 6. Regeneration at relatively low flow rates (test case 3).

Good agreement between experimental and computed values implies insignificant temperature gradients along the filter.

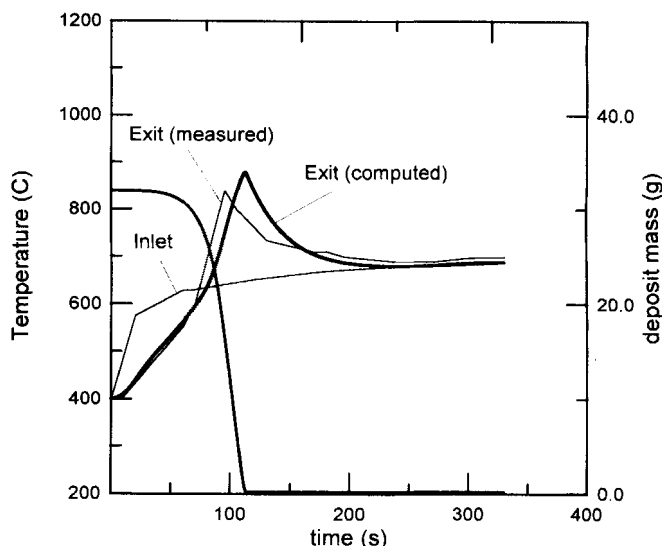


Figure 7. Regeneration at high initial loading (test case 4).

generation case, in order to identify the critical trends in a more concise and general way.

An idealized regeneration process with constant feed gas temperature and flow rate will be analyzed. The trap is supposed to be thermally equilibrated with the exhaust gas at the beginning of the regeneration. Perfect soot oxidation to  $\text{CO}_2$  is also assumed. The physical properties of the ceramic filter are taken equal to that of cordierite with 50% porosity. In the present case, we are interested in the maximum temperature  $T_{\max}$  developed during the regeneration process, as well as the total regeneration duration  $t_{\max}$ . The dimensions of the physical magnitudes involved in this regeneration process are expressed in the technical system as  $[\text{Force}]^m [\text{Length}]^n [\text{Time}]^o [\text{Temperature}]^p$  as shown in Table 3.

According to the Buckingham's  $\Pi$ -theorem, we can formulate  $8 - 4 = 4$  dimensionless numbers ( $\Pi$ -groups), that adequately describe the phenomenon. The numbers selected for this purpose are

$$\bar{w} = \frac{w_b}{w_s} \quad (28)$$

$$Dam = \frac{m_b}{F(0)} \frac{1}{t_{\text{reaction}}} \quad (29)$$

$$\bar{T}_{\max} = \frac{T_{\max}}{T_i} \quad (30)$$

Table 3. Physical Magnitudes and Dimensions of the Idealized Regeneration Process for the Dimensional Analysis

	Force	Length	Time	Temp.
$F$	1	-1	1	0
$\rho_g$	1	-4	2	0
$T_i$	0	0	0	1
$T_{\max}$	0	0	0	1
$w_b$	0	1	0	0
$w_s$	0	1	0	0
$t_{\max}$	0	0	1	0
$t_{\text{reaction}}$	0	0	1	0

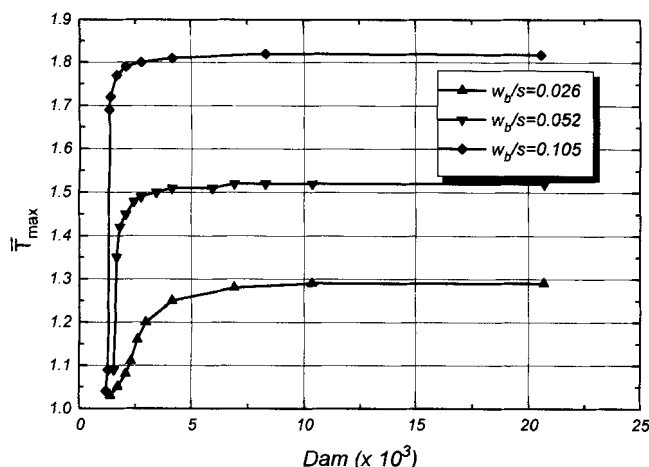


**Figure 8. Dimensionless maximum temperature during the idealized regeneration process.**

$$\bar{t}_{max} = \frac{F(0)}{m_b} t_{max} \quad (31)$$

After execution of a number of model simulations with variable input parameters and using the dimensionless numbers derived above, the dimensionless regeneration duration and maximum temperature can be plotted as functions of the Damköhler number with  $\bar{w}$  as independent parameter. Some interesting conclusions may be drawn from the interpretation of these graphs.

For a given filter, the maximum temperature developed is merely a function of the initial soot loading for Damköhler numbers above  $5 \times 10^{-3}$ , which become higher for higher initial loading. On the other hand, a filter with thicker walls is subjected to lower temperature peaks for the same initial soot loading. Figure 8 clearly shows the existence of a critical Damköhler number, under which regeneration “freezes”. This number is, moreover, only slightly dependent on the  $\bar{w}$  values lying in the range of interest. We can get some physical explanations for this if we look at the variables appearing in the

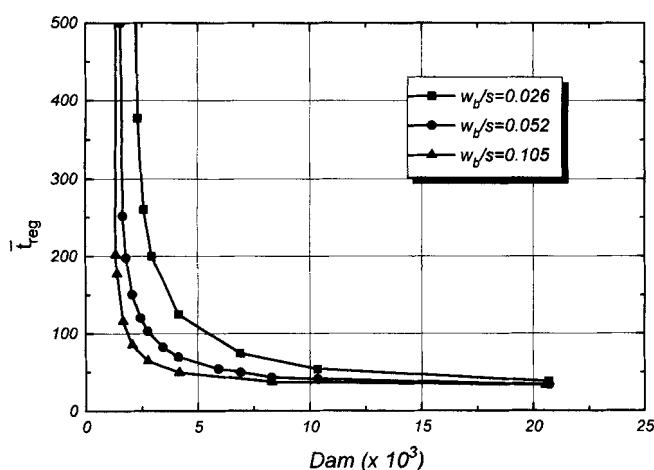


**Figure 9. Dimensionless regeneration duration during the idealized regeneration process.**

Damköhler number. The regeneration can be retarded or even frozen, when one or more of the below occurs:

- The feed gas temperature is too low.
- The oxygen content of the feed gas is too low.
- The residence time of the feed gas in the soot layer is too low. This may either occur due to high exhaust gas flow rates or due to low filter loading.

Analogous conclusions can be drawn from Figure 9 showing the regeneration duration as function of *Dam*. The critical *Dam* leading to infinite regeneration durations is also recognized, whereas for *Dam* higher than  $5 \times 10^{-3}$  the dimensionless duration approaches a constant value of about  $40 \times 10^{-3}$  practically independent of  $\bar{w}$ .

Most of the above mentioned conclusions drawn from the dimensionless presentation of model results are widely common to the experienced engineers in the field. The described method merely aims at a more concise representation of the well-known trends and interactions involved in the thermal regeneration process.

### Model Applications: Regeneration Rate Control

The durability of regenerable trap systems probably presents the major obstacle in their wider application in vehicle applications. Filter failure may either result from overheating above the melting point or from local high temperature gradients that cause severe thermal and mechanical stresses. This occurs under several failure scenarios, a typical one comprising of an engine operation at high load and subsequent braking leading to idle operation with low exhaust flow rates. It is necessary to develop regeneration control strategies in order to eliminate reaction rates during a failure scenario. Considering the well-known behavior of the regeneration process and keeping in mind the theoretical results presented in the previous section, we can state four major approaches for limiting the undesired high regeneration rates:

- Maintaining low mean trap loading
- Cooling of the filter
- Reduction of the exhaust gas oxygen content
- Decreasing the exhaust gas residence time in the soot layer.

Apart from the first one, the above approaches may have the secondary effect of increasing the regeneration duration. The above theoretical possibilities could be realized in practice by the following techniques:

- Limiting trap loading by controlling regeneration frequency
- Limiting oxygen availability by controlling A/F,
- Limiting oxygen availability by keeping a low exhaust flow rate
- Filter cooling by keeping a high exhaust flow rate.

Real-world application of all four directions requires special control algorithms. The design of control systems for such applications is supported significantly by the model presented in this work. In this section, these techniques will be briefly investigated with the aid of theoretical model predictions. It must be mentioned that the only evaluation criterion is the maximum temperature developed during regeneration, as the zero-dimensional model cannot provide any statements about local temperature gradients in the filter.

In regard to the effect of trap loading on the regeneration safety, Figure 8 may provide some hints. Namely, in the range of sufficiently high Damköhler numbers the maximum filter temperature is affected directly by trap loading. Thus, a design criterion for fixing the maximum permissible loading level for a given allowable filter temperature is already established.

The principle of trap protection by limiting the oxygen content of the feed exhaust gas has recently been shown to be effective for a number of trap failure scenarios (Pattas et al., 1995). This technique is expected to be supported by new developments in exhaust gas sensor and electronic signal processing technologies. Keeping the oxygen content low at any engine operating points may be accomplished by controlled exhaust gas recirculation (EGR), whereas tight control of the A/F ratio (directly connected to  $O_2$  content) requires use of accurate and fast responding exhaust gas oxygen sensors. The determination of the "safe" A/F for the control of the regeneration process at various operating points is a fairly complicated task.

Figure 10 shows the predicted trap temperatures developed during a failure scenario comprising a sudden vehicle braking following engine operation at high load and speed. The parameters used for the simulation of such a scenario are given in Table 4, and are characteristic for conditions met in passenger car applications. The evolution of the exhaust gas feed temperature during the operation mode change is a function of the thermal response properties of the parts intervening between the engine and the trap. Data regarding the trap filter are given in Table 1. A fairly high trap loading of 35 g and an initial trap temperature of 550°C are selected for the simulation.

The regeneration in this case already begins during phase I, but becomes steeper when shifting to phase II ( $t = 20$  s). When no A/F control is imposed on the engine, the maxi-

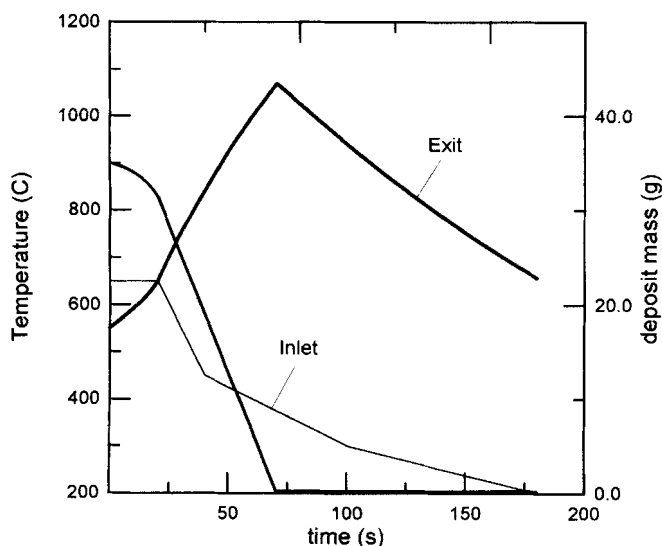


**Figure 10.** Model results for the simulation of an uncontrolled regeneration during a trap failure scenario.

Parameters data are given in Table 1 and Table 4. The high trap temperatures developed would apparently lead to trap failure in real-world conditions.

**Table 4. Model Parameters Used as Input for the Simulation of a Trap Failure Scenario**

Phase	Temp. °C	Mass Flow Rate kg/s	$O_2$ Conc. %
I	650	50	5
II (idle)	200	10	15

mum trap outlet predicted temperature overrides 1,000°C. According to experience from analogous observed cases, such outlet temperatures usually accompany a local filter overheating which has already been led to local filter melting.

The feasibility of protecting the trap by limiting the oxygen content in the exhaust gas is illustrated in Figure 11. It is clear that the regeneration becomes slower with lower oxygen content, as expected since the soot oxidation rate is directly proportional to oxygen concentration. The regeneration is, however, still hazardous even at oxygen concentrations of 7%, whereas the value of 4% seems to be the safe limit for the specific case.

As another possibility, limiting available oxygen for the regeneration is already employed in a number of bypass regen-

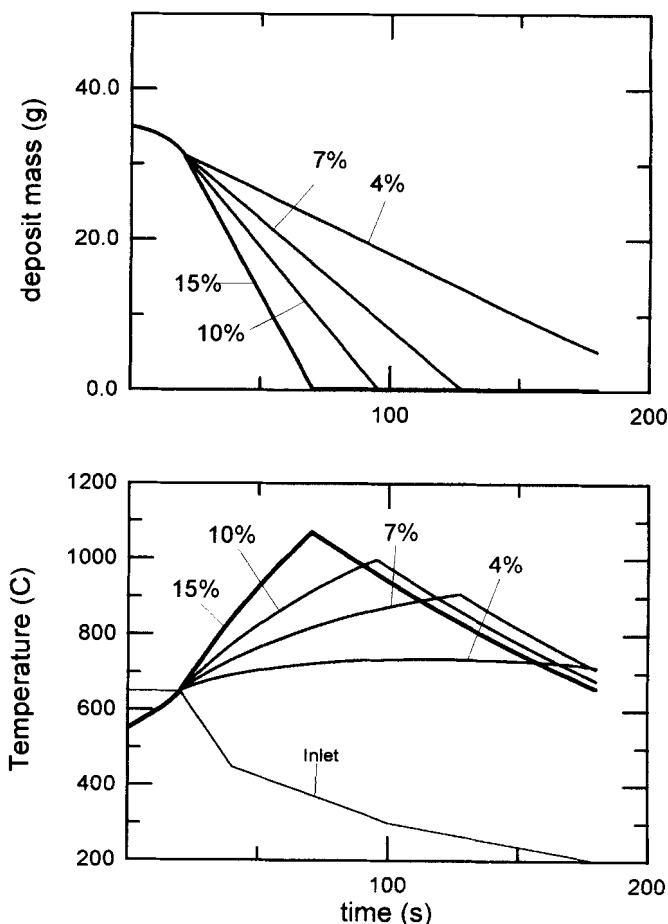


**Figure 11.** Trap protection by limiting the exhaust gas oxygen content during regeneration (controlled regeneration).

The trap outlet temperature is compared for different oxygen concentrations.

eration systems (Kumagai et al., 1992; Kojetin et al., 1993). This technique is very well suited for externally assisted regeneration systems (such as electrically heated burners). A trade-off between regeneration duration (which should not be very high) and maximum filter temperature must be accounted for in such systems. Model computations are indispensable design tools in this case.

The opposite approach, namely very much increasing exhaust flow rate per unit filter volume is another possibility to assure safe regeneration. Extensive simulation with a model is necessary to successfully design and tune such a trap protection system.

For example, one could refer to the full flow regenerable, burner assisted trap system described in Huehn and Sauerteig (1989). The principle of operation of trap protection in this class of systems relies upon a compressor that is capable of sustaining sufficiently high flow rate through the trap even at idle conditions. The determination of additional air flow required for safe regeneration, as a function of the engine operation point with the maximum permissible trap loading as parameter, can be aided substantially by computational simulation of the type represented in Figure 8 and Figure 9.

## Other Application Areas

In the previous section the capability of the model to cope with a full class of design problems related to trap safety has been demonstrated. Naturally, the use of the model may be extended to a variety of other design problems.

A very interesting research and development area that could profit very much from modeling trap operation is the application of traps in turbo-charged diesel engines (Pattas and Stamatelos, 1991, 1992; Mayer et al., 1994). In the class of systems with the trap before turbine the necessity exists to minimize trap heat capacity and improve the design of the exhaust system before the trap in order to maintain an acceptable trap exit temperature response. Thus, it is necessary to follow a systems approach in the design of the system aiming at diminishing the difference in response between engine out and trap exit temperatures (Figure 2a).

Another critical aspect of trap modeling applications is related to the increasing concern on on-board diagnostics (OBD) for emission control systems in all vehicle types (Koltsakis and Stamatelos, 1995). Due to special aspects of the design of trap systems (wide variety of filter types with significantly varying filtering efficiencies regarding the solid and soluble organic fraction of the particulate, also varying with engine operation point, etc.), it is absolutely necessary to computationally support any OBD development efforts.

Finally, trap models of the type presented in this article may be widely used in the sizing of trap systems, provided that they are equipped with reliable pressure drop computation submodels. It may be stated that the development of diesel particulate traps for vehicular applications has already entered the stage of computationally assisted systems design approach.

## Conclusions

Future stricter emission standards render it necessary to investigate the rationale of developing reliable trap systems

for a wider range of vehicular applications. Although the thermal regeneration of wall-flow filters has been studied extensively, the use of mathematical models to support system optimization has been relatively limited.

The feasibility of employing a control-oriented zero-dimensional modeling approach for this purpose is studied in this article. A sound mathematical model is used as a starting point and is further developed in the direction of providing better agreement with experimental observations. The formation of carbon monoxide from incomplete soot oxidation seems to play an important role in the evolution of the regeneration process and should be taken into account in the model equations.

Estimation of trap loading—a critical parameter for modeling applications—is shown to be possible by an integrated energy balance, based on simple temperature recordings during regeneration. Suitable tuning of the reaction kinetic constants can be attained with the help of a comprehensive set of full-scale experiments.

Following the above steps, the comparison of model predictions with experimental measurements showed promising results for a variety of regeneration conditions tested. The correlation was poorer when significant temperature gradients in the axial or radial direction of the filter existed. The dimensional analysis of an idealized regeneration process provided a more concise presentation of the relative significance of the model parameters.

The model is already used by the authors to support the optimum design of regeneration control techniques aiming at more durable trap systems. Future work in the field includes a deeper investigation of CO formation during regeneration, chemical kinetics of soot oxidation at very low oxygen concentrations, as well as application of the existing approach to the modeling of the use of catalysts to assist the regeneration process.

## Notation

- $A$  = filtration area,  $m^2$
- $A/F$  = air to fuel mass ratio
- $\bar{C}_{p1}$  = dimensionless heat capacity,  $C_{p1} \rho_1 / (C_{p2} \rho_2)$
- $C_{p2}$  = specific heat capacity of exhaust gas,  $1,090 \text{ J/kg} \cdot \text{K}$
- $C_{p1}$  = specific heat capacity of soot deposit,  $1,510 \text{ J/kg} \cdot \text{K}$
- $C_{p2}$  = specific heat capacity of ceramic wall,  $1,120 \text{ J/kg} \cdot \text{K}$
- $Dam$  = Damköhler number,  $m_b / [F(0)t_{reaction}]$
- $E$  = apparent activation energy of soot oxidation,  $150 \times 10^3 \text{ J/mol}$
- $\bar{F}$  = dimensionless exhaust gas mass-flow rate,  $F(t)/F(0)$
- $F(t)$  = mass-flow rate of exhaust gas,  $\text{kg/s}$
- $F(0)$  = value of  $F(t)$  at  $t = 0$
- $\Delta H$  = "combined" reaction enthalpy of soot oxidation,  $\text{J/mol}$
- $\Delta H_{(i)}$  = specific heat of  $\text{CO}_2$  formation,  $3.61 \times 10^5 \text{ J/mol}$
- $\Delta H_{(ii)}$  = specific heat of  $\text{CO}$  formation,  $0.90 \times 10^5 \text{ J/mol}$
- $k_j$  = dimensionless rate coefficient,  $(s_1 w_b A p M_a k_j) / [RT_b F(0)]$
- $k_j$  = rate coefficient for the reaction in region  $j$ ,  $\text{m/s}$
- $k$  = collisions frequency factor,  $6.0 \text{ m/s} \cdot \text{K}$
- $m$  = accumulated soot mass,  $\text{kg}$
- $M_a$  = molecular weight of exhaust gas,  $29 \times 10^{-3} \text{ kg/mol}$
- $M_c$  = atomic weight of deposit,  $12 \times 10^{-3} \text{ kg/mol}$
- $\bar{M}$  = molecular weight ratio
- $p$  = exhaust gas pressure,  $101 \times 10^3 \text{ Pa}$
- $R$  = gas constant,  $8.31 \text{ m}^3 \cdot \text{Pa/mol} \cdot \text{K}$
- $s_1$  = specific area of deposit layer,  $5.5 \times 10^7 \text{ m}^{-1}$
- $t$  = time,  $\text{s}$
- $\bar{t}$  = dimensionless time,  $F(0)t/m_b$
- $T$  = temperature,  $\text{K}$
- $\bar{T}$  = dimensionless temperature,  $T/T_b$

$T_b$  = temperature at  $t = 0$ , K  
 $T_i(t)$  = inlet temperature, K  
 $\bar{T}_i$  = dimensionless inlet temperature,  $T_i/T_b$   
 $t_{\text{reaction}}$  = characteristic reaction time,  $\rho_1/(s_1 \rho_s k_j y_i)$ , s  
 $v$  = superficial velocity, m/s  
 $w$  = thickness of the deposit layer, m  
 $\bar{w}$  = dimensionless deposit layer thickness,  $w/w_b$   
 $w_s$  = channel wall thickness, m  
 $\bar{w}_s$  = dimensionless wall thickness,  $w_s/w_b$   
 $x$  = distance, m  
 $\bar{x}$  = dimensionless distance,  $x/w_b$   
 $y$  = oxygen concentration of the exhaust gas (mole fraction)  
 $y_i(t)$  = mole fraction of oxygen at inlet

## Greek letters

$\Delta P$  = trap backpressure, Pa  
 $\epsilon$  = dimensionless group  $C_{pg} F(0) w_b / A \lambda_1$   
 $\lambda$  = bulk thermal conductivity  
 $\bar{\lambda}_j$  = ratio of thermal conductivities,  $\lambda_j/\lambda_1$   
 $\rho$  = exhaust gas density, kg/m<sup>3</sup>  
 $\rho_1$  = bulk density of the deposit layer, 550 kg/m<sup>3</sup>  
 $\rho_2$  = bulk density of porous ceramic, 1,400 kg/m<sup>3</sup>

## Subscripts

$b$  = initial condition  
 $i$  = inlet condition

## Literature Cited

- Aoki, H., A. Asano, K. Kurazono, K. Kobashi, and H. Sami, "Numerical Simulation Model for the Regeneration Process of a Wall-Flow Monolith Diesel Particulate Filter," SAE paper 930364 (1993).  
 Bissett, E. J., "Mathematical Modeling of the Thermal Regeneration of a Wall-Flow Monolith Diesel Particulate Filter," *Chem. Eng. Sci.*, **39**(7/8) 1233 (1984).  
 Bissett, E. J., and F. Shadman, "Thermal Regeneration of Diesel-Particulate Monolithic Filters," *AIChE J.*, **31**(5), 753 (May, 1985).  
 De Soete, G., "Combustion Catalytique des Sues Formees en Phase Gazeuse a Partir de Diesel-Oils," Institut Francais du Petrole-Techniques d'Applications Energetiques, Rapport IFP No. 35378 (1987).  
 Frohne, J., H. Reisig, and K. Schaedlich, "Thermoanalytische Methoden zur Charakterisierung von Dieseleruss," *Wissenschaft & Technik*, **42**(4), (April 1989).  
 Garner, C. P., and J. C. Dent, "A Thermal Regeneration Model for Monolithic and Fibrous Diesel Particulate Traps," SAE paper 880007 (1988).  
 Higuchi, N., S. Mochida, and M. Kojima, "Optimized Regeneration Conditions of Ceramic Honeycomb Diesel Filter," SAE paper 830078 (1983).  
 Hoepke, E., "Partikelfilter fuer Omnibusse und Kommunalfahrzeuge," *Automobile Technische Zeitschrift (ATZ)*, 91 s. 680., 12 (1989).  
 Hoffman, U., and J. Ma, "Study on Regeneration of Diesel Particulate Filter Using a Laboratory Reactor," *Chem. Eng. Tech.*, **13**, 251 (1990).  
 Howitt, J. S., and M. R. Montierth, "Cellular Ceramic Diesel Particulate Filter," SAE paper 810114 (1981).  
 Huehn, W., and J. E. Sauerteig, "The New DEUTZ Particulate Trap System for Trucks and Buses," SAE paper 892494 (1989).  
 Johnson, J. H., S. T. Bagley, L. Gratz, and D. Leddy, "A Review of Diesel Particulate Control Technology and Emission Effects," SAE paper 940233 (1994).  
 Kojetin, P., F. Janeszich, L. Sura, and D. Tuma, "Production Experi-

- ence of a Ceramic Wall Flow Electric Regeneration Diesel Particulate Trap," SAE paper 930129 (1993).  
 Koltsakis, G. C., and Stamatelos, A. M., "Detection of Automotive Catalyst Failure by Use of On-Board-Diagnostics," *J. Automotive Eng., Proc. of IMechE*, **209**, 171 (1995).  
 Kumagai, Y., Y. Kono, and T. Ideda, "A Particulate Trap System Using Electric Heating Regeneration for Small Trucks," SAE paper 920141 (1992).  
 Lepperhoff, G., and G. Kroon, "Abgasnachbehandlung I— Verminderung der Partikelemission von Dieselmotoren fuer PKW durch Abgasnachbehandlung," Abschlussbericht, Vorhaben Nr. 259, Heft 352, FVV (1984).  
 Lox, E. S., B. H. Engler, and E. Koberstein, "Diesel Emission Control," *Catalysis and Automotive Pollution Control II*, A. Crucq, ed., Elsevier Science Publishers B.V., Amsterdam (1991).  
 Mayer, A., R.-M. Schmidt, H. Sudmanns, and B. A. Mattes, "Pre-Turbo Application of the Knitted Fiber Diesel Particulate Trap," SAE paper 940459 (1994).  
 McCabe, R. W., and R. M. Sinkevitch, "A Laboratory Combustion Study of Diesel Particulate Containing Metal Additives," SAE paper 860011 (1986).  
 Merrion, D. F., *Diesel Engine Design for the 1990s*, SAE publication SP-1011 (1994).  
 Moser, F., E. Haas, and H. Schloegl, "Zur Partikelemission von Nutzfahrzeug-Dieselmotoren," *Motor Techn. Zeitschrift*, 51 (1990).  
 Pattas, K. N., A. M. Stamatelos, K. N. Kougianos, G. C. Koltsakis, and P. K. Pistikopoulos, "Trap Protection by Limiting A/F during Regeneration," SAE paper 950366 (1995).  
 Pattas, K. N., and C. C. Michalopoulou, "Catalytic Activity in the Regeneration of the Ceramic Diesel Particulate Trap," SAE paper 920362 (1992).  
 Pattas, K. N., and A. M. Stamatelos, "Transient Behaviour of Turbo-Charged Engine Vehicles Equipped with Diesel Particulate Traps," SAE paper 920361 (1992).  
 Pattas, K. N., and A. M. Stamatelos, "A Trap Oxidizer System for the Turbo-charged Diesel Engine," SAE paper 910137 (1991).  
 Pattas, K. N., and Z. C. Samaras, "Computational Simulation of the Ceramic Trap Transient Operation," SAE paper 890403 (1989).  
 Pattas, K., Z. Samaras, N. Patsatzis, C. Michalopoulou, O. Zogou, A. Stamatelos, and M. Barkis, "On-Road Experience with Trap Oxidiser Systems Installed on Urban Buses," SAE paper 900109 (1990).  
 Pauli, E., E. Lepperhoff, and F. Fischinger, "The Calculation of Regeneration Limits of Diesel Particulate Traps for Different Regeneration Methods," SAE paper 840075 (1984).  
 Rao, V. D. N., and H. A. Cikanek, "Diesel Particulate Control System for Ford 1.8L Sierra Turbo Diesel to Meet 1997–2003 Particulate Standards," SAE paper 940458 (1994).  
 Shadev, R., V. Wong, and S. Shahed, "Analysis of Regeneration Data for a Cellular Ceramic Particulate Trap," SAE paper 840076 (1984).  
 Stamatelos, A. M., "Impact of Environmental Legislation on the Design of Vehicle Diesel Engines: The Case of Diesel Particulate Traps," ASME/NTU Athens '91 International Conference, Athens (1991).  
 Wade, W., J. White, J. Florek, and H. Cikanek, "Thermal and Catalytic Regeneration of Diesel Particulate Traps," SAE paper 830083 (1983).  
 Walton, F. B., E. K. Bueckert, D. P. Archambault, and R. W. Kempster, "On-Line Measurement of Diesel Particulate Loading in Ceramic Filters," SAE paper 910324 (1991).  
 Weaver, C. S., "Particulate Control Technology and Particulate Standards for Heavy Duty Diesel Engines," SAE paper 840174 (1984).  
 Wiedemann, B., U. Doerges, W. Engeler, and B. Poettner, "Regeneration of Particulate Filters at Low Temperatures," SAE paper 830086 (1983).

Manuscript received Apr. 24, 1995, and revision received Aug. 24, 1995.